Electron Microscopy and Diffraction Studies on the Growth and Structure of Laminar Single Crystals of Colloidal Gold (Special Issue on Electron Microscopy)

AUTHOR(S):

Suito, Eiji; Uyeda, Natsu

Electron Microscopy and Diffraction Studies on the Growth and Structure of Laminar Single Crystals of Colloidal Gold

Eiji SUITO and Natsu UYEDA*

(Suito Laboratory, Institute for Chemical Research, Kyoto University)

Received January 20, 1965

When dilute aqueous solution of auric chloride is reduced under an acidic condition, small plate-like crystals grow forming triangular, hexagonal or other polygonal shapes in the suspension. These crystals were identified to be single crystals of gold by electron microscopy and selected area diffraction. The lattice orientation of the crystal was determined by means of dark field image analysis and it was revealed that the flat habit surface was (111) plane of the f.c.c. lattice of gold. The size of the plate ranges from a few microns to some ten microns in diameter and the thickness is about 100 Å in an average as determined by the analysis of subsidiary maxima of diffraction spots. Anomalous diffraction spots that were observed in many cross grating patterns were interpreted in terms of the thickness of the crystal lamellae.

Spiral growth steps were also observed on both faces of a lamella with small holes at the core of screw dislocations which were located at the center of spiral loop. The relationship between the hole diameter and the expected strength of Burgers vector was examined on the basis of Frank's theory and the effective strength of the Burgers vectors turned out to be the same order as the step height of the growth spiral.

The growth process was also examined, and very irregularly indented perimeters were found on every crystal which was on growth in the suspension. Indentation of various kinds was classified into several morphological groups. Dark contrast band of about 1000 Å in width was observed at the periphery of each crystal with irregular indentation. This was attributed to the imperfections in the newly formed part of the crystal. The indentation is considered to be due to the adsorption of a small ordinary colloidal gold and also to the further rearrangement of the lattice after the adsorption. The deposition with atomic order can not be ruled out for the explanation of the growth of these laminar crystals of colloidal gold.

The present paper is a review of those works as were previously carried out in the authors' laboratory.

INTRODUCTION

It has long been known that the colloidal solution of gold contains very fine particles of gold which are stably dispersed in it. Although the optical microscope was useful for the verification of the existence of such particles and also for the indirect measurement of particle sizes, the electron microscope was the first to reveal their definite morphological aspects. Among the ordinary particles which were as round as used to be anticipated, von Borries and Kausche[1] found some triangular and hexagonal ones in their electron micrograph of colloidal gold which was prepared by Zsigmondy's method. The size of these polygonal particles was small and rather comparable with that of ordinary round ones of around 500 mμ in average diameter. Later, Suito and Arakawa[2] also found similar polygonal particles in Zsigmondy sol which was prepared as the speci-

* 水渡英二，植田　夏

men to determine the resolving power of the electron microscope. Stevenson, Turkevich and Hiller[3] studied the rate of nucleation in the reactant solution and found polygonal laminar particles by means of electron microscopy.

Suito and Uyeda[4] independently studied the influence of the pH of the solution upon the size of resulting particles. In this case, dilute solution of chloroauric acid was reduced with hydrogen peroxide solution and the total pH was controlled with varied amount of potassium carbonate solution in advance of the addition of the reducing reagent.

The result showed that the particle size was increased as the initial pH of the solution tended toward acidic as is shown in Table 1. It was also anticipated from this results

Table 1. *The influence of pH on the particle size of resulting colloidal gold.*

$HAuCl_4$* (ml)	K_2CO_3** (ml)	pH	Particle Size (mμ)
61.3	—	5.4	30-100 (80)***
61.3	1.2	5.6	25-100 (75)
61.3	2.4	6.4	30-70 (60)
61.3	3.2	7.2	8-60 (45)
61.3	4.0	8.2	-30 (30)
61.3	4.7	9.4	10-50 (25)

* $HAuCl_4$: 0.025%
** K_2CO_3 : 0.1 N
*** The values in the parentheses are the mean values.

that the particle would grow even larger when the pH was further shifted toward strongly acidic side. This was simply achieved by the addition of hydrochloric acid so that the final pH of the solution was decreased down to 2.3. It turned out by electron microscopy that the resulting particles were extraordinarily large and thin, and also that they took various morphological aspect. Miura and Tamamushi[5] also observed laminar particles which were prepared by the reduction of pure chloroauric acid solution with salicylic acid. Oberlin[6] studied the epitaxial growth of similar crystals on thin molybdenum sulfide and graphite crystals. Brüche[7] showed that these crystals sometimes grew so large that the average diameter was measured to be more than 60 μ. The strong acidic condition under which these laminar particles appeared was far out of the desirable range of pH for the ordinary stable colloidal gold to be obtained. Moreover, the particles are so large that they are easy to settle down to the bottom of the container of the solution. But still, they showed very interesting aspect in regard to the growth mechanism and, on the other hand, they have always been very suitable specimens to improve the technique of the electron diffraction microscope which in turn has been playing an important role in the investigation of thin crystalline films. Recently, Chiang and Turkevich[8] studied the growth mechanism of such laminar gold platelets and had excellent agreement with those obtained by the present authors.

Preparation of Gold Sol

Various methods for the preparation of the ordinary sol were invented so far. In

the present case, however, the following special methods were applied.

(1) A small quantity of dilute HCl solution was added to the dilute aqueous solution of auric chloride (0.06 %) so that the final pH of the solution was decreased to 2.5 or less. The solution was then reduced with 3 % H_2O_2 solution after about 10 minutes boiling.

(2) The same aqueous solution of auric chloride was reduced with a few ml. of saturated salicylic acid solution.

When the reaction temperature was high, the resulting particle were rather thick and small. Thus, in order to obtain thinner crystals which were suitable for the diffraction work, the solution was kept at room temperature all the time until the growth of laminar crystals was completed, although it took a week or ten days for the reaction to come to an end.

The light also seemed to have a considerable effect for the reaction and further growth to proceed, because when the glass vessel in which the reacting solution was contained was kept in the total darkness, the reaction was detained to a considerable extent or sometimes it never took place at all. At the outset of the reaction, the solution was yellow and transparent. As the reaction proceeded, however, the total solution became turbid and the color turned into reddish brown in reflecting light and blue in transmitting light. When the turbidity came to a point beyond which no more change was observed, the reaction was considered to be completed.

The specimens for the practical electron microscopy was prepared by putting a small droplet onto specimen grids which were covered beforehand with supporting film of Formvar or collodion.

The Morphology of Laminar Crystals of Gold[9]

It was revealed by the electron microscopy that the shapes most frequently assumed by these laminar crystals of colloidal gold were (A) triangle, (B) hexagon and (C) intermediate polygon of the two, as shown in Fig. 1, which is a reproduction of typical examples of the classified electron micrographs. Besides these typical ones, there appeared less frequently some laminar crystals with more irregular shapes, as shown in Fig. 1 (D), (E) and (F). A simple geometric examination of these shapes shows that the individual crystal has a trigonal symmetry around an axis which is normal to the large habit face on which the crystal itself lies. It will be interesting to notice that even the most complicated crystal in Fig. 2 a, also show the same symmetry, as is illustrated in Fig. 2 b. With such a corolla-like form, three pairs of parallel lines can always be assigined crossing one another at an angle θ of exactly 120°. This means that the retardation of the growth front made the outlook somewhat complicated but the crystal habit itself is essentially the same as the others like (B) and (C) in Fig. 1. The size of the crystal is distributed over a wide range. The average value of the magnitude is about 3-5 mincrons in diameter of the circumscribed circle of the regular polygon. The thickness is estimated from the results of shadow casting method to be about 100 Å in an average. Although it is well known that the contrast of the electron images changes according as the glancing angle of the crystal to the incident electron beam, the present laminar crystals of colloidal

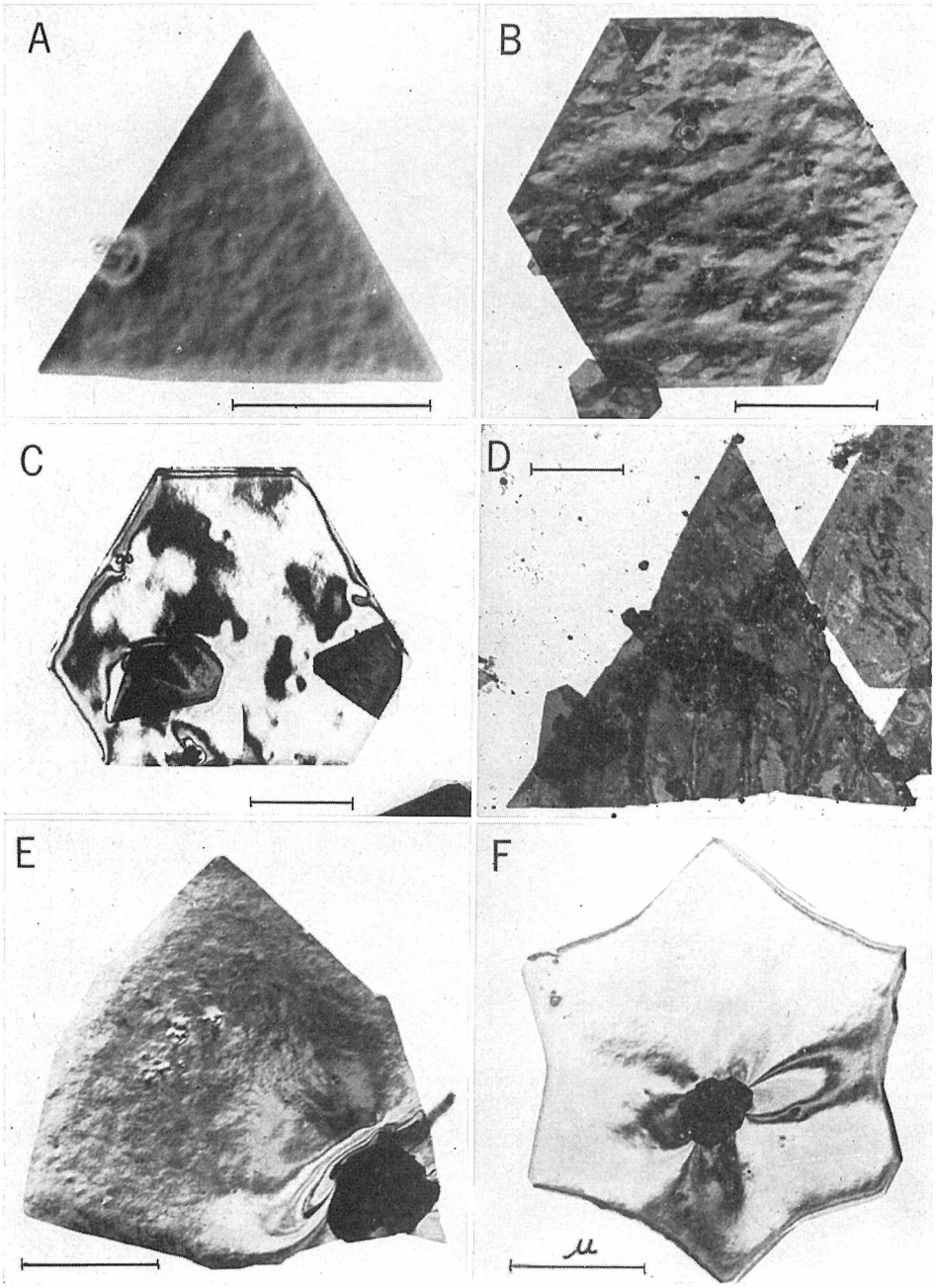

Fig. 1. Various outward apperances of laminar single crystals of acidic colloidal gold.

gold is always very thin and is generally transparent to the electron beam. One of the most precise method of determining the thickness of such crystalline lamellae is to rely upon the anlysis of the subsidiary maxima of electron diffraction spots. The detail will be discussed later.

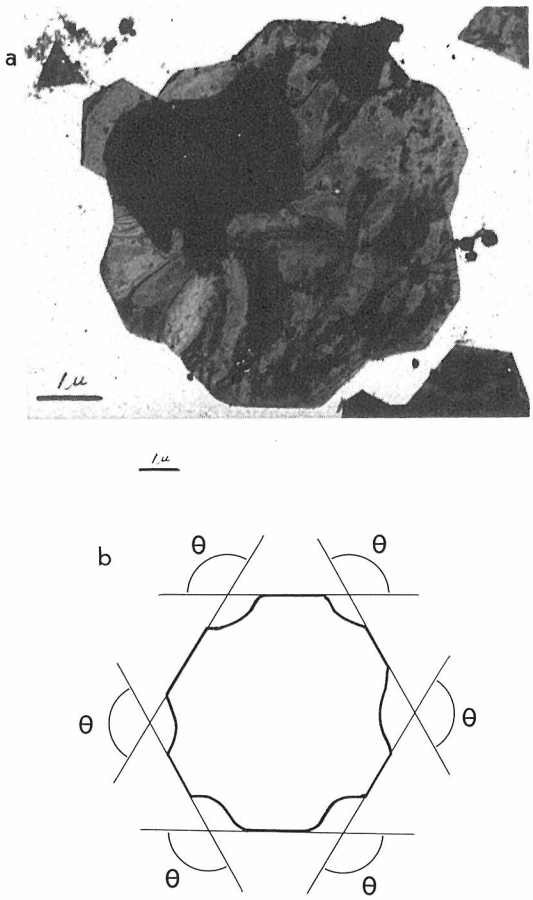

Fig. 2. Coro"a-like form and its symmetry.

The complicated striped contrast which are observed on the habit surfaces are not always essential character of these crystals, but mostly due to the electron optics which has a close connection to the diffraction effects, as was first pointed out by Heidenreich[10]. The detail will also be discussed later in regard to the lattice orientation in the crystal.

Identification of the Laminar Crystals by Electron Dffraction

By the application of the high resolution electron diffraction, sharp Debye-Scherrer rings were obtained from a considerably wide area of the specimen grid to identify the laminar crystals. The standard electron diffraction pattern was prepared by the use of a vacuum evaporated thin film of metallic gold. The example of both patterns is reproduced in Fig. 3 (A) and (B). The coincidence of these two are very good except for these rings as (200) and (400) rings which are missing in the pattern from the laminar crystals. When the specimen grid was deeply tilted against the incident electron beam, these missing rings were detected as shown in the fiber pattern in C. It is obvious from these facts that these laminar crystals are nothing but gold and

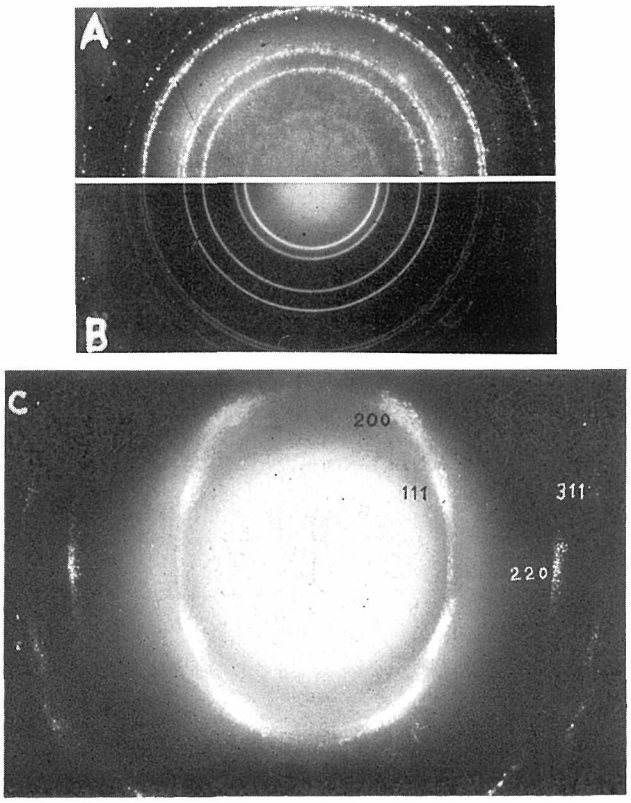

Fig. 3. Electron diffraction patterns obtained from
A: laminar single crystals of colloidal gold
B: vacuum evaporated gold film
C: the same specimen as A at a tilted orientation.

show a rather perfect orientation on the supporting film, the details of which will be discussed in the next section.

Determination of the Lattice Orientation in the Crystal

Since gold has a face centered cubic lattice, where the trigonal symmetry axis appears in the [111] direction, it will be obvious that the flat habit surfaces of these laminar crystals are to be assigned as the (111) plane. This presumption was also proved on the basis of some results obtained by the selected area electron diffraction as shown in Fig. 4 and the dark field image analysis[11].

The main purpose of the selected area electron diffraction is to obtain directly the diffraction pattern from a particular area of the specimen by the use of an intermediate lens and an intermediate diaphragm of variable aperture size with which the given area to be examined is selected. This method was applied to the laminar single crystal of colloidal gold, that was mounted on a specially curved specimen grid as shown in Fig. 5 so that individual crystals would take various orientations and glancing angles to the incident electron beam[12]. From a single crystal a cross-grating patterns can be obtained and the variation of the orientation to the incident electron beam also changes the

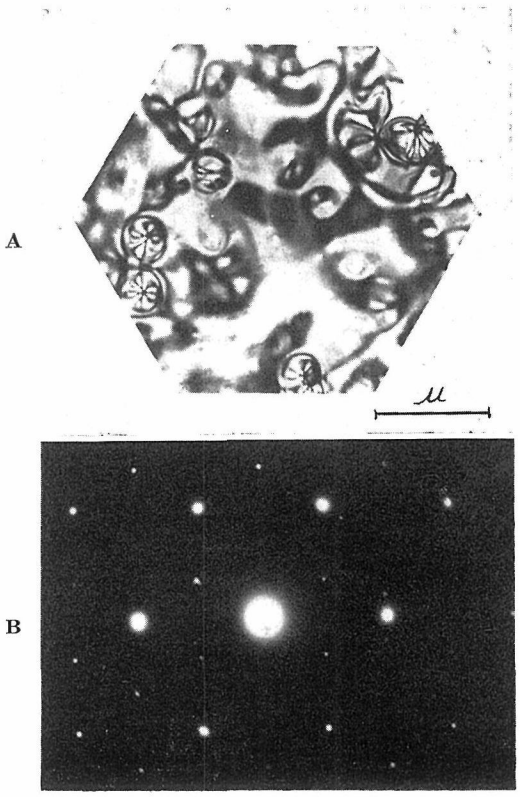

Fig. 4. A laminar single crystal of colloidal gold and its selected area electron diffraction pattern with hexagonal symmetry.

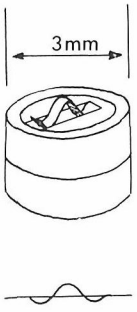

Fig. 5. Special specimen grid that furnishes varying inclination to the specimen crystals.

resulting cross-grating pattern, depending on the direction as well as the amount of the inclination of the single crystal to the incident beam. Some examples of the cross-grating patterns thus obtained are reproduced in Fig. 6 together with the associated electron micrographs of the gold crystals. Fig. 6 (A) was obtained when the electron beam passed through the crystal with a normal incidence to the flat habit surface of the crystal. The symmetry is perfectly trigonal. It is worth-while to compare this pattern

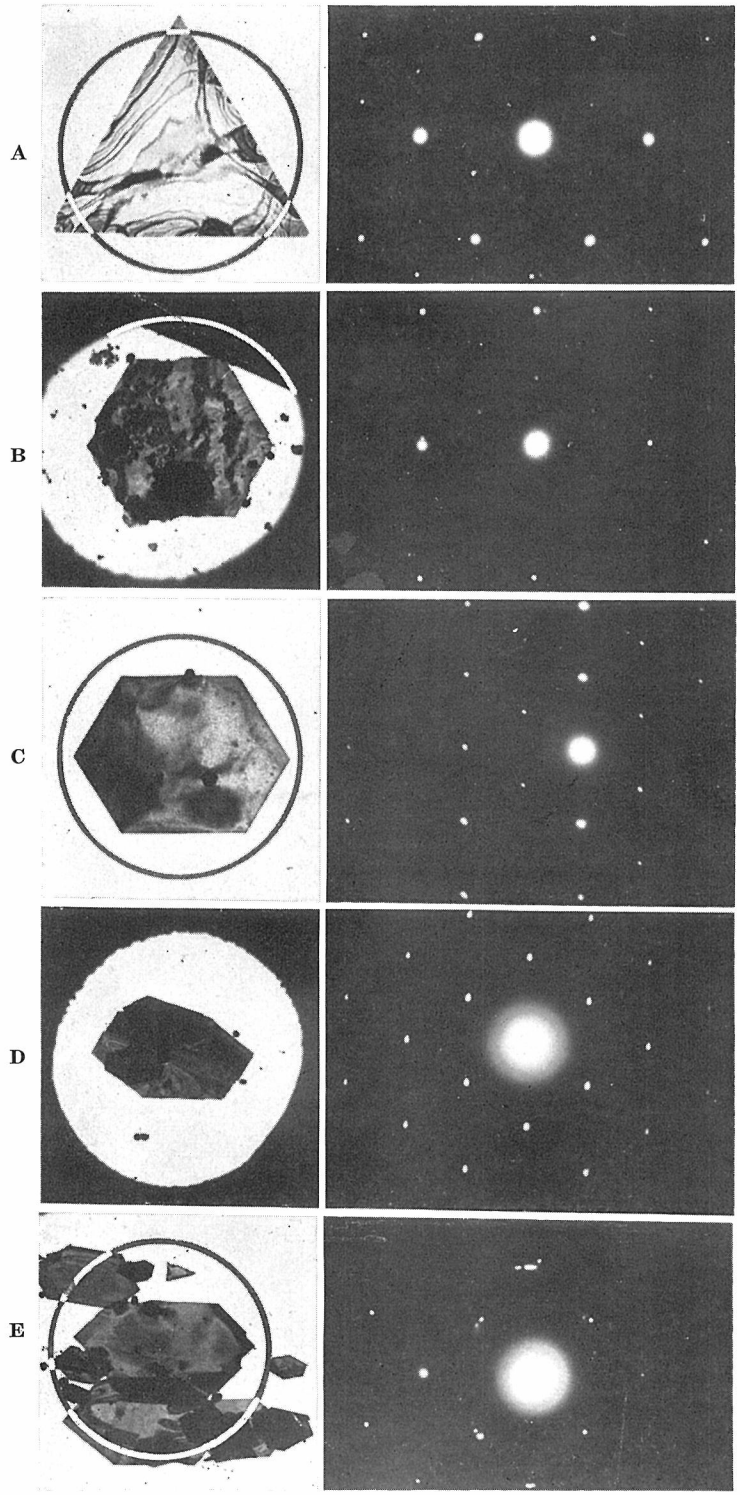

Fig. 6. Laminar single crystals of colloidal gold and selected area electron diffraction patterns at various inclinations (The diameter of each circles is 3 μ).

with the ordinary Debye-Scherrer rings an example of which has been shown in Fig. 3. To make this comparison simple, a specimen of similar colloidal gold was prepared with an additional evaporated thin film of gold on it. The selected area electron diffraction gave rise to a superimposed pattern of Debye-Scherrer rings and a cross grating pattern as shown in Fig. 7. The six main diffraction spots of (220) group exactly fit on the

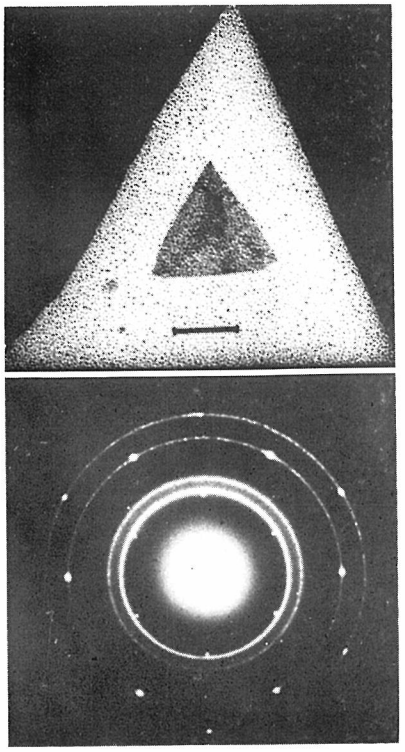

Fig. 7. A hexagonal cross grating pattern of single crystal and superimposed Debye-Scherrer rings of evaporated film of gold. (Taken by R. Ueda)

Debye-Scherrer ring of the same index. However, other six weak spots which are supposed to be the ones from (111) group are not superimposed upon the associated ring but show a slight shift toward inside of the ring. Moreover, the intensity is not as strong as is supposed to be. This is due to the thinness of the crystal lamella and can be interpreted in terms of the reciprocal lattice and the Ewald sphere.

Since the original lattice structure is face-centered cubic, the reciprocal lattice of gold is assigned to be a body-centered cubic lattice, in which the [111] axis of the original lattice passes through the body diagonal direction of the cubic unit cell of the reciprocal lattice, that is, the direction which connects the origin and the total (hhh) points. Moreover, when it is assumed that the original crystal is very thin in the direction of the same [111] axis, the intensity regions which are associated with individual reciprocal lattice points are elongated along the same [111] direction because of the decrease along this

direction in the number of unit cell which will act as the diffraction grating for the electron wave. The total appearance of such a reciprocal lattice which consists of these lattice points with intensity regions elongated along the [111] direction is schematically shown in Fig. 8 as a projection to a diagonal plane of a cube that includes the [111] axis.

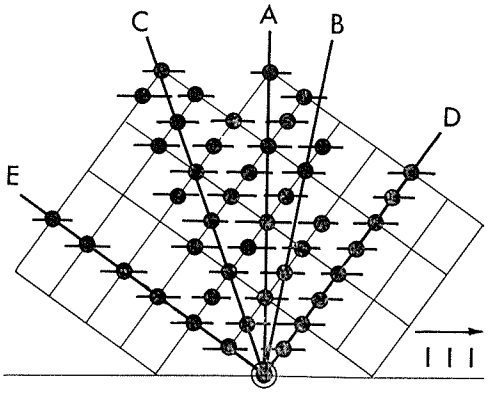

Fig. 8. The reciprocal lattice of laminar single crystal of gold that shows elongation of intensity regions toward [111] direction, and Ewald spheres at various inclinations.

In the case of the high energy electron diffraction, the Ewald sphere can be approximated by a plane which passes through the origin of the reciprocal lattice with a normal parallel to the incident electron beam. And a section of the reciprocal lattice with Ewald sphere gives rise to the electron diffraction pattern which is antcipated when the electron beam hits the crystal at the same mutual orientation. The thick lines in Fig. 8, which are designated by A, B, C, D and E show the various orientation of the Ewald sphere at the same sequence as that of Fig. 6. In all cases the Ewald spheres are normal to the same plane to which the reciprocal lattice was projected. As to A, which is for the normal incidence of the electron beam, the Ewald sphere cuts the reciprocal lattice with the six main points of (220) group on it, whereas it never hits the (111) points but only the elongated intensity regions of these points. It is obvious from this result that the diffraction spots due to the (111) reflection always appeares with a shorter radius than that of the real reflection in case of the normal incidence. By a simple geometric relationship the amount of this shift is given to be 5.22 %. In the orientation A, the Ewald sphere cannot cut the points that belong to (2n,00) group. This is the reason why the reflections due to (200), (400) and so on are absent in the diffraction pattern obtained under an ordinary condition.

The other examples of diffraction patterns in (B) to (E) can also be interpreted on the basis of the same model concerning the elongation of intensity regions and the orientation of the Ewald sphere. The angle between the normal to the crystal habit surface and the incident electron beam can be calculated graphically with each electron micrograph of the single crystal gold by measuring the apparent edge angles which are supposed

to be 60° or 120° if not tilted. These angles showed good agreement with those that are described for individual orientations of the Ewald sphere in Fig. 8. And the electron diffraction patterns also showed good coincidences with the schematic patterns which are geometrically anticipated from the intersections of the reciprocal lattice given by the individual orientations of the Ewald sphere as shown in Fig. 8. It will be interesting to notice that the diffraction spots for the (2n,00) group appear in the pattern (C) and (D) which was obtained at such deep glancing angles of about 35 to 55°. Now that it seems reasonable from these results to assign the flat habit surface to be the (111) plane, it is also worthwhile to determine another crystal axis to fix the total orientation of the lattice in the crystal. To achieve this determination, the method of dark field image analysis was applied to a single crystal which showed somewhat regular networks of extinction contor lines as shown in Fig. 9. These contor lines are known to be due to the diffraction effect[10]. When the crystal has some warping, the inclination of a lattice plane

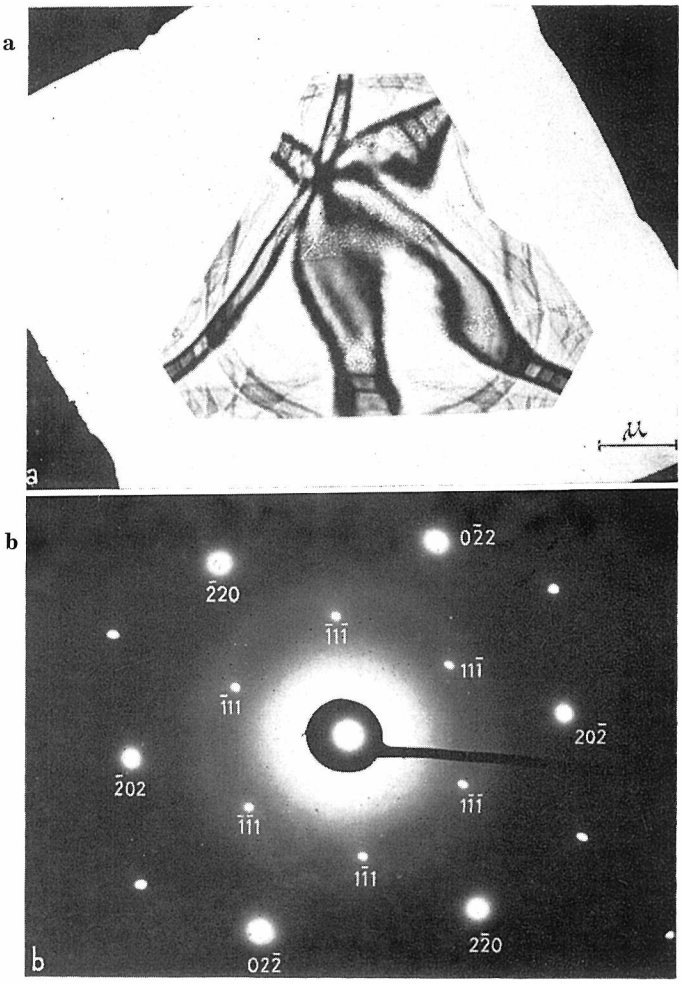

Fig. 9.

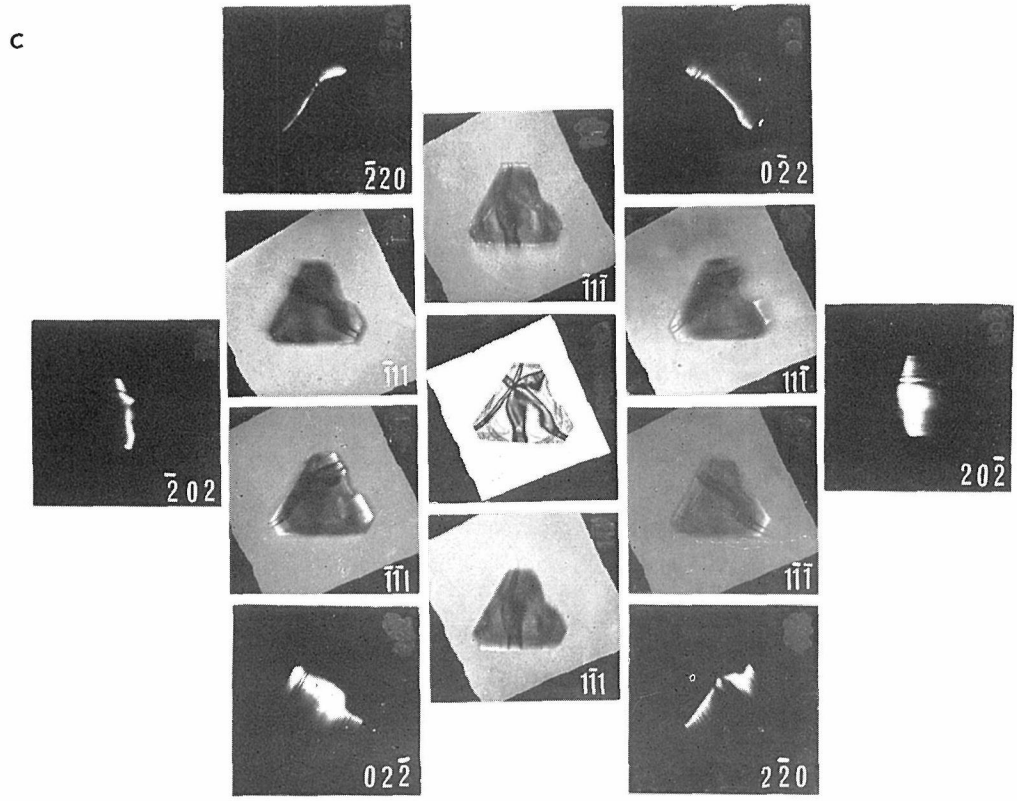

Fig. 9. Dark field image analysis of extinction contor lines for the determination of the lattice orientation in the crystal.

to the electron beam varies from place to place even in the same crystal. At some places where the angle of the plane just satisfy the Bragg condition for diffraction, the electron beam is reflected and stopped by the objective aperture which is ordinarily located at the principal plane of the objective lens. Thus, when the final electron image is formed on the screen with only the scattered electron which passed through the small objective aperture, the local place where the electron was reflected appears as a dark extinction contor lines. On the contray, when a dark field image is formed by moving the objective aperture aside and letting each reflected beam pass through it, one can obtain a dark field image which corresponds to the dark contor lines in the bright field image[13]. The set of dark field images in Fig. 9 (c) were obtained by this method with each diffraction spots shown in Fig. 9 (b) which is the selected area diffraction pattern of Fig. 9 (a). With the direction in which the contor lines of (220) groups run taken into account, the orientation of the total lattice in the crystal was easily determined as shown in Fig. 10.

The Determination of the Thickness by the Analysis of Subsidiary Maxima

As mentioned above, one of the most precise methods to determine the thickness of thin laminar crystalline materials is to anylize the subsidiary maxima of diffraction spots. Fig. 11 shows some elongated diffraction spots, split into a series of subsidiary

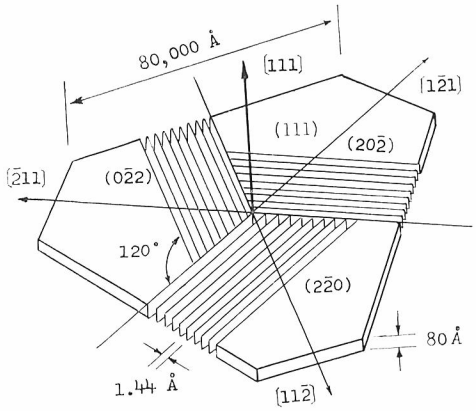

Fig. 10. Total morphological aspect and lattice orientation of a laminar single crystal of colloidal gold.

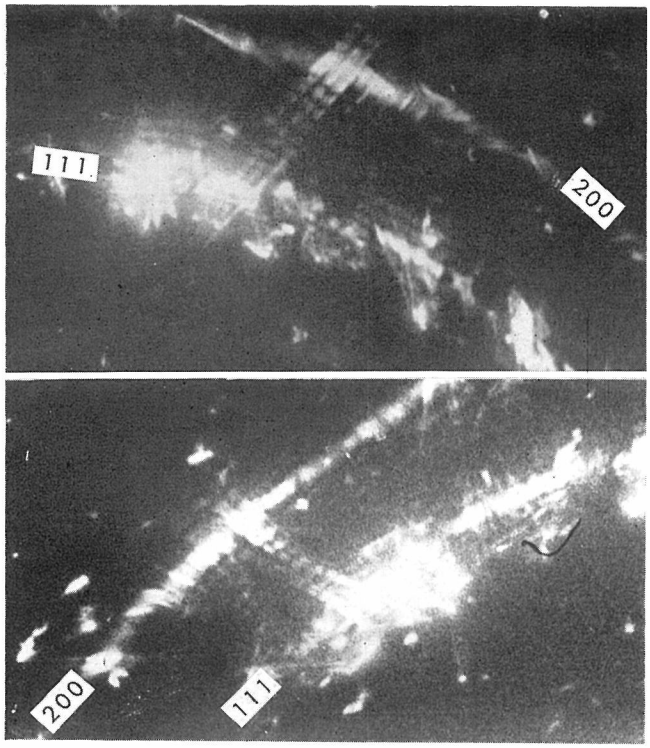

Fig. 11. Subsidiary maxima in the high resolution electron diffraction spots obtained from laminar single crystals of colloidal gold.

spots, which were found in the Debye-Scherrer rings obtained from similar single crystals of colloidal gold. The displacement of these spots from the main one that precisely satisfies the Bragg condition has a close relation to the thickness of the original crystal.

For the interpretation and the analysis of these subsidiary spots, it is again convenient to consider the relationship between the reciprocal lattice and the Ewald sphere. The elongated intensity region in the direction normal to the habit surface has periodic maxima which are defined by the diffraction function ϕ_L as schematically shown in Fig. 12. When

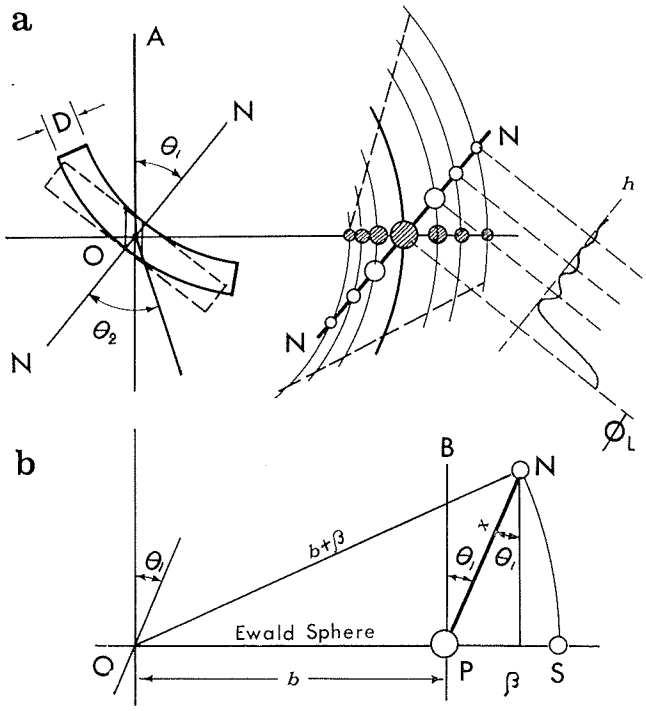

Fig. 12. The schematic diagram of the analytical method of subsidiary maxima.

the positions of these maxima are represented by a series of point which are located on the elongation of the intensity region (NN′) and the original crystal bends around an axis parallel to the surface, the resulting rotation of the total reciprocal lattice around its origin causes these points to draw concentric circles. When the Ewald sphere cuts through the point (hkl) the sections of these circular loci appear as the subsidiary maxima in the diffraction spots in the "elongation" like Fig. 11. From Fig. 12 b, the periodic factor h_n of the maxima is given by the relationship[14],

$$h_n = d_N \left\{ \sqrt{\frac{\sin^2\theta_1}{d^2} + \frac{2\Delta\theta}{\lambda d} + \frac{(\Delta\theta_n)^2}{\lambda^2}} - \frac{\sin\theta_1}{d} \right\}, \tag{1}$$

where d = the interplanar spacing of (hkl) planes

h_n = the angular displacement of the n-th subsidiary maximum ($n = 2m+1$) from the principal maximum,

θ_1 = the angle between the normal of the flat habit face and the incident electron beam

d_N = the interplanar spacing of the lattice plane parallel to the flat habit face.

Hashimoto[15] established an equation that relates the thickness, the periodicity of the subsidiary maxima, the Fourier potential of the lattice plane, etc. on the basis of the dynamical theory of electron diffraction developed by Bethe[16]. The relationship between the thickness D and the periodicity h is given by

$$h_n = \pm\left[\left(\frac{nd_N}{2D}\right)^2 - \left\{\frac{d_N V_N}{\lambda E\sqrt{(\cos\theta_1 \cos\theta_2)}}\right\}^2\right]^{1/2} \qquad (2)$$

where E is the accelerating voltage of the electron beam, V_N is the Fourier potential of the lattice plane by which the diffraction takes place, and θ_2 is the angle between the normal to the flat habit face and the diffracted electron beam. Thus, by measuring the angular diaplacements $\Delta\theta_n$ with the subsidiary maxima in Fig. 11, the periodic factor h_n can be obtained, which in turn is available to obtain the thickness D in terms of the Eq. (2). As an unknown value V_N is included in Eq. 2, it is of course necessary to use at least two h_n values obtained from Eq. (1).

About ten or more examples of the elongated spots were examined on (111), (200) and (311) rings and the values of angular displacements were calculated with Eq. 1. The thickness D and the corresponding number of unit cells $M(=D/d_N)$ were also calculated with Eq. (2). In the present case, the flat surface is the (111) plane and the interplanar spacings d_N is 2.35 Å. The results of the calculation shown in Table 2

Table 2.

(*hkl*)	$\Delta\theta_n \times 10^4$	h_n	M	D(Å)	h_n'	M'	D'(Å)
(111)	2.03	0.026	35	82.3	0.027	32	75.2
	5.12	.063			.068		
	3.78	.047	39	91.7	.049	35	82.3
	5.73	.069			.076		
	4.72	.058	23	54.1	.062	20	47.0
	8.88	.103			.117		
	2.33	.030	49	115.2	.031	45	103.4
	4.15	.051			.055		
	2.79	.035	39	91.7	.037	36	84.6
	5.07	.062			.067		
	2.80	.035	47	110.5	.037	42	98.7
	4.85	.055			.064		
	4.66	.057	26	61.1	.061	22	51.7
	8.31	.096			.109		
(200)	6.53	.049	32	75.2	.050	31	72.9
	10.71	.079			.082		
	3.73	.028	45	105.8	.029	44	103.4
	7.00	.052			.053		
	5.07	.038	35	82.3	.039	34	79.9
	9.33	.069			.071		
(311)	2.77	.078	19	44.7	.087	15	35.3
	5.05	.130			.016		
		M.V.	35	83.1	M.V.	32	75.4

indicate that the laminar single crystals of colloidal gold are very thin, and that the thickness ranges from 40 to 120Å even with these examples that were incidentally extracted. However, these results are in reasonable agreement with that roughlly estimated by the shadow-casting method.

Spiral Growth of Laminar Single Crystal of Colloidal Gold

Many examples of the growth spiral have been reported since Frank[17] introduced the idea of screw dislocation into the general mechanism of crystal growth. Amelinckx[18] has observed the spiral growth step on electrochemically deposited gold crystal. Very conspicuous spiral growth steps were also observed on the laminar single crystals of colloidal gold[19 20]. Similar phenomena were also observed independently by Rang and Poppa[21] on colloidal gold crystals of the same kind, whereas Brüche and Demny[7] made a discussion on the growth mechanism of these crystals.

i) Various kinds of spiral growth steps. One of the most typical and ordinary examples of spiral marking is shown in Fig. 13 where a crystal lamella with a shape of near-

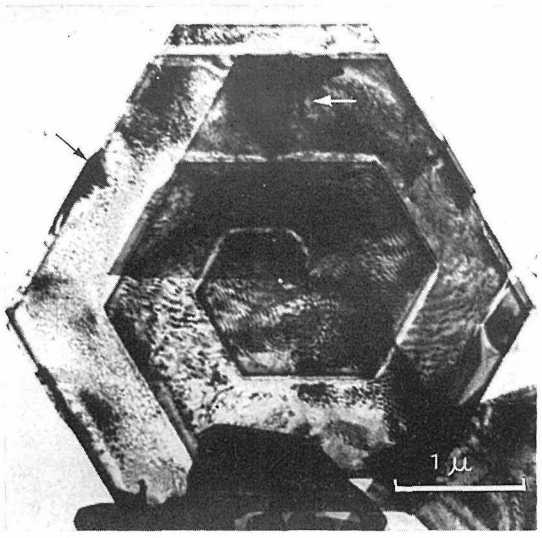

Fig. 13. A laminar single crystal of colloidal gold with a typical spiral growth loop.

ly regular hexagon can be observed. Starting from the center of the crystal, the growth spiral also makes a hexagon loop, which leaves the spiral steps of nearly equal width on the flat habit surface of the (111) plane. The complicated stripe patterns are ascribed to moiré fringes. A series of electron micrographs of various kinds of superimposed spiral steps are reproduced in Fig. 14 with schematic diagrams for some of them to distinguish the actual loop of the steps. The average number of turns of these loops around the center of the spiral is not large but only three to five in most cases.

In the present work, since the specimen was prepared in the suspension, it seems reasonable that the spiral growth would take place on both surfaces on a single lamella,

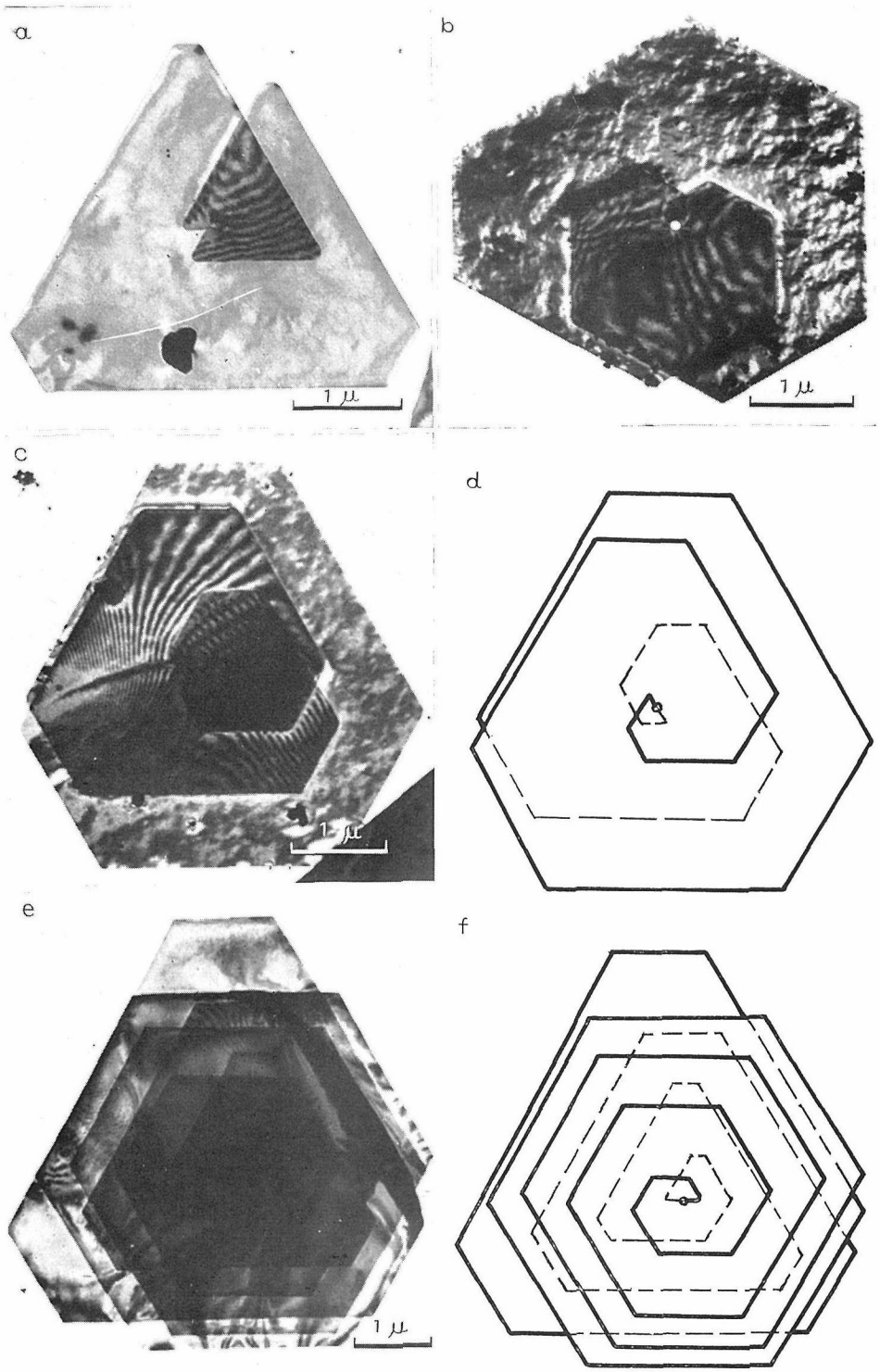

Fig. 14. Various spiral steps with single source.

if the core of screw dislocations, the Burgers vector of which is normal to the habit face, entirely passes through the lamella with its two ends on both surfaces. A similar phenomenon has also been reported by Amelinckx and Votava[22] on the crystal of $K_4Fe(CN)_6$ which grew on the surface of the solution, but the condition and the process of the crystal growth were different from those of the present case. In the present gold crystals, the couple of growth spirals can be observed at the same time by electron microscopy as well shown in the series of photographs in Fig. 14, since the step is about 100 Å on an average and is almost tranparent to the electron beam even when 7 to 10 steps are superimposed together. In the schematic illustration in Fig. 14 the thick lines show the spiral steps on one surface and the broken ones are for those on the opposite surface. This situation can also be confirmed by the use of shadow casting method or the technique of the carbon replica. In both cases, the aspect of only top surface can be well revealed. Fig. 15 shows an example of these carbon replica, which were obtained by dissolving

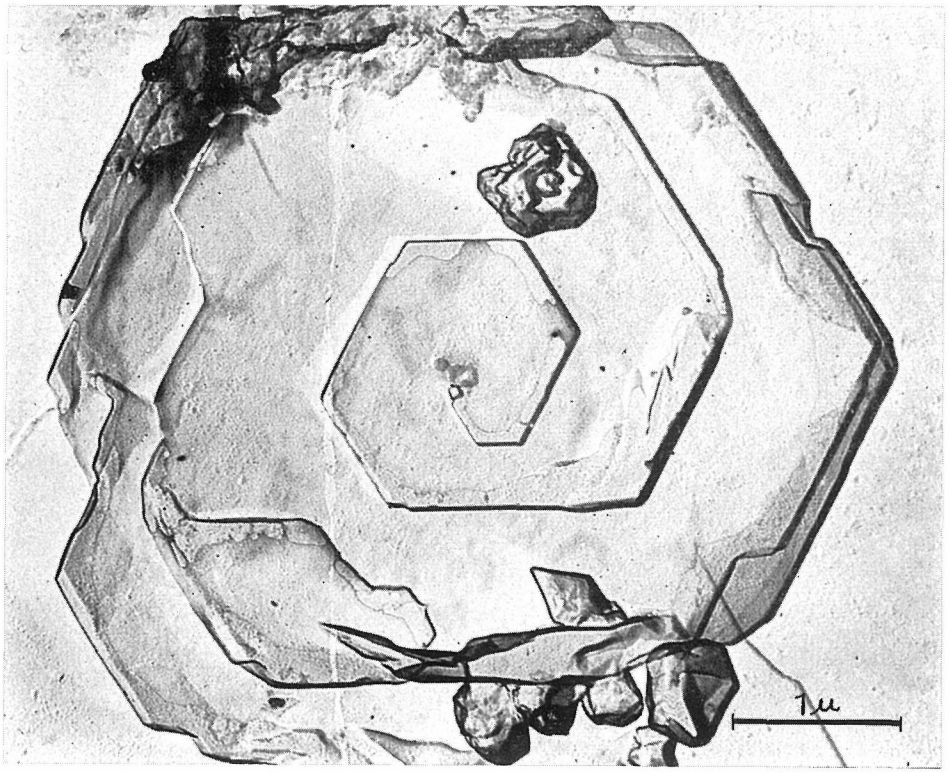

Fig. 15. Carbon replica that shows the spiral loop of one face of the gold crystal.

the gold crystals with aqua regia after the carbon film was vacuum deposited on the top of the gold crystals.

With the above observations, a three dimensional configuration of such a crystal that has double spiral steps can be suggested as illustrated in Fig. 16 which shows a lateral view of the crystal, although the step height is slightly exaggerated. The couple of arrows in the figure show the position of the core of screw dislocations. The two

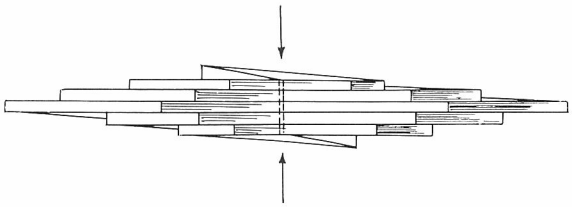

Fig. 16. A lateral view of the gold crystal with spiral steps on both faces of the lamella.

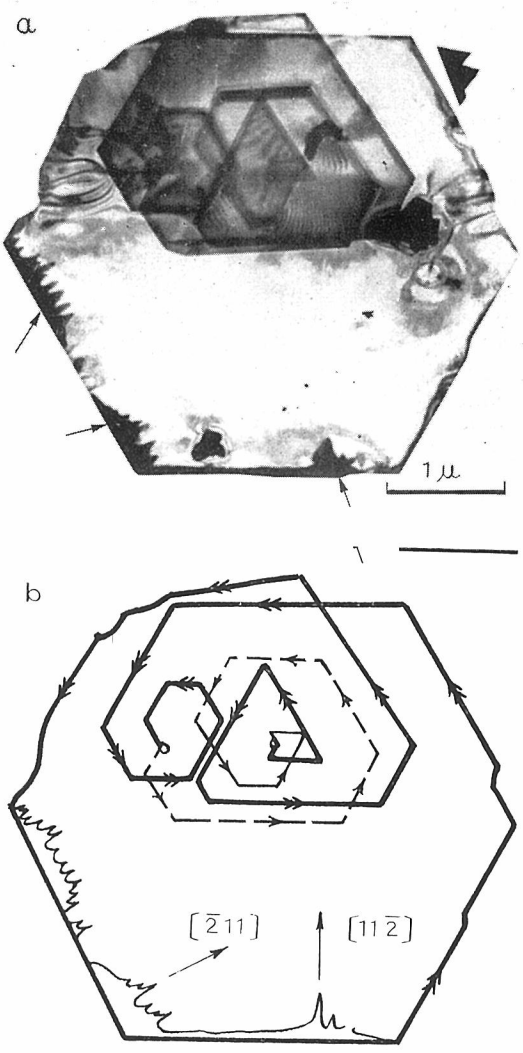

Fig. 17. A laminar gold crystal with two sources of spiral loops.

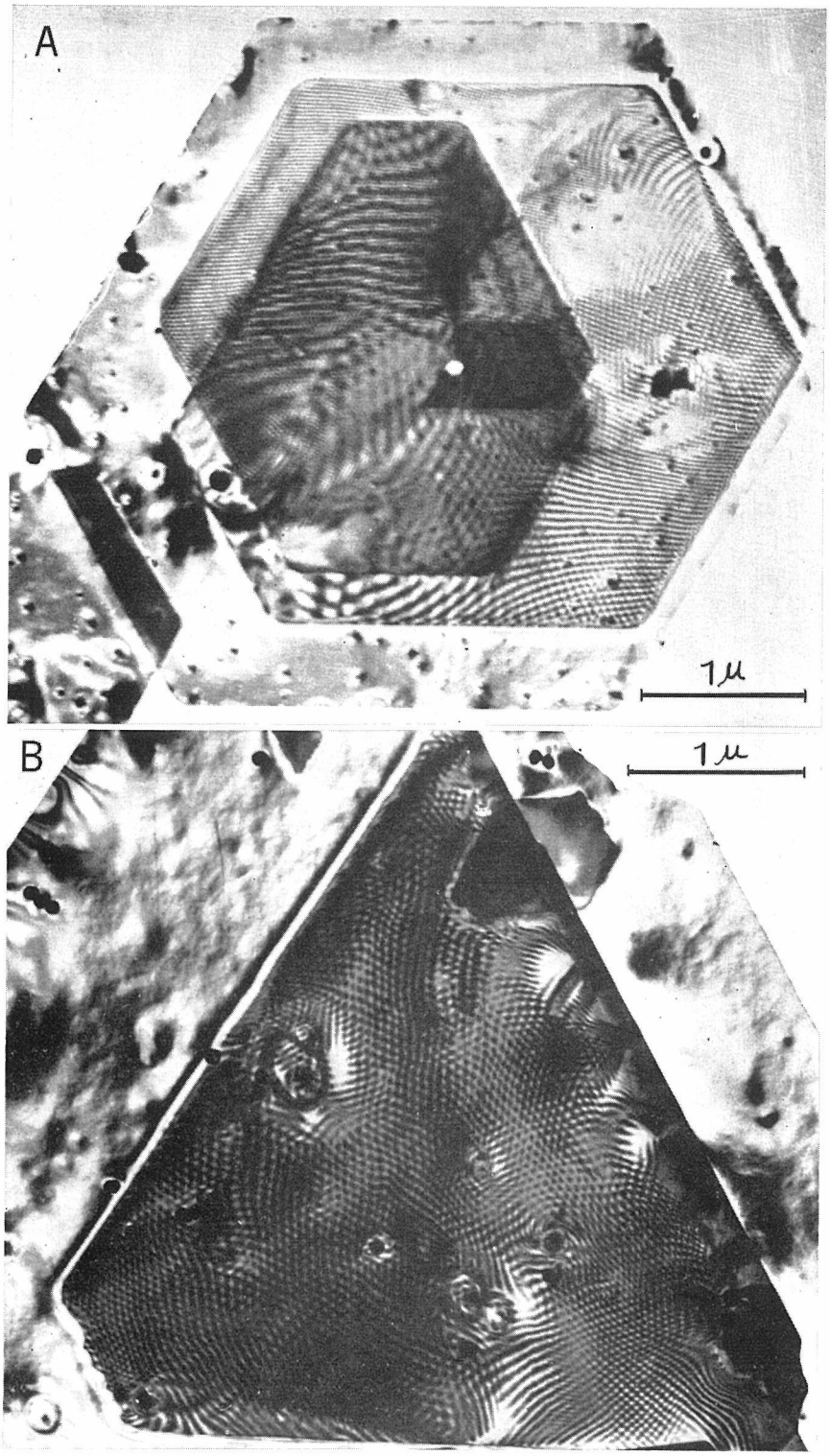

Fig. 18. Various moiré patterns that appeared on the superimposed part of spiral steps.

spirals on both surfaces are nearly symmetric in most cases. This is very reasonable as the specimens have grown in the suspension and the condition of the medium must have been the same on both sides of each crystal during the growth.

In Fig. 17, another example of spiral steps is shown together with its schematic diagram of spiral loop, where two sources of growth spiral can be observed. One spiral loop, originated from one source, terminates at another source as illustrated with thick line, whereas the other loop, starting from the latter source goes into the former source as shown with broken lines. The three dimensional configuration is much more complicated than that of a single source.

ii) Various kinds of fringed pattern and the rotation of spiral steps. The complicated patterns observed on the habit surfaces of the crystals are ordinary extinction fringes or the moiré patterns, the latter of which essentially appears on the places where more than two growth steps are superimposed. The patterns became more and more complicated as the number of the superposition of the steps is increased as shown in Fig. 18. The appearance of these moiré fringes on the superimposed part of the spiral steps are considered to be due to the rotational misorientaton between these steps around an axis normal to the flat habit surface.

Fig. 19 is a set of electron micrographs which include a laminar gold crystal with a hexagonal spiral loop and the series of dark field images formed with the reflected beams, the indexes of which are respectively designated in the patterns. The small angle of rotation between the steps can be roughly estimated on the basis of an assumption that the origin of these moiré patterns is ascribed only to the rotational misorientation. The angle of rotation s is given by the following equation:

$$s = M \cdot d/D \tag{3}$$

where d and M are the interplanar spacing of the lattice plane, the reflection of which caused the moiré fringe of a width D, and the total magnification of the dark field images. The s was calculated at various positions of the steps and was plotted against the angular position on the step starting from the tentative origin and following up the loop toward the center of the spiral. The result is shown in Fig. 20 where the actual spacings of the moiré fringes are also plotted. The quantity of such rotational misorientation is an order of 10^{-4} to 10^{-3} rad. However, it will be worth noting that the misorientation is much larger at the center of the spiral where it is reasonably accepted that the distortion caused by the core of scew dislocations seems to have an important effect on such a misorientation.

iii) The small holes at the center of the growth spiral. Small holes of various size were very often observed at the center of the spiral. Fig. 21 shows some of the enlarged photograph of these centers with the hole. The shape of the hole is nearly hexagonal in most of the cases, although the edge of the hexagon are somewhat rounded in. The edge line of the hole is always parallel to that of the loop line. The spiral loop starts from one of the rounded apexes of the hole with a curved line at the outset. Since

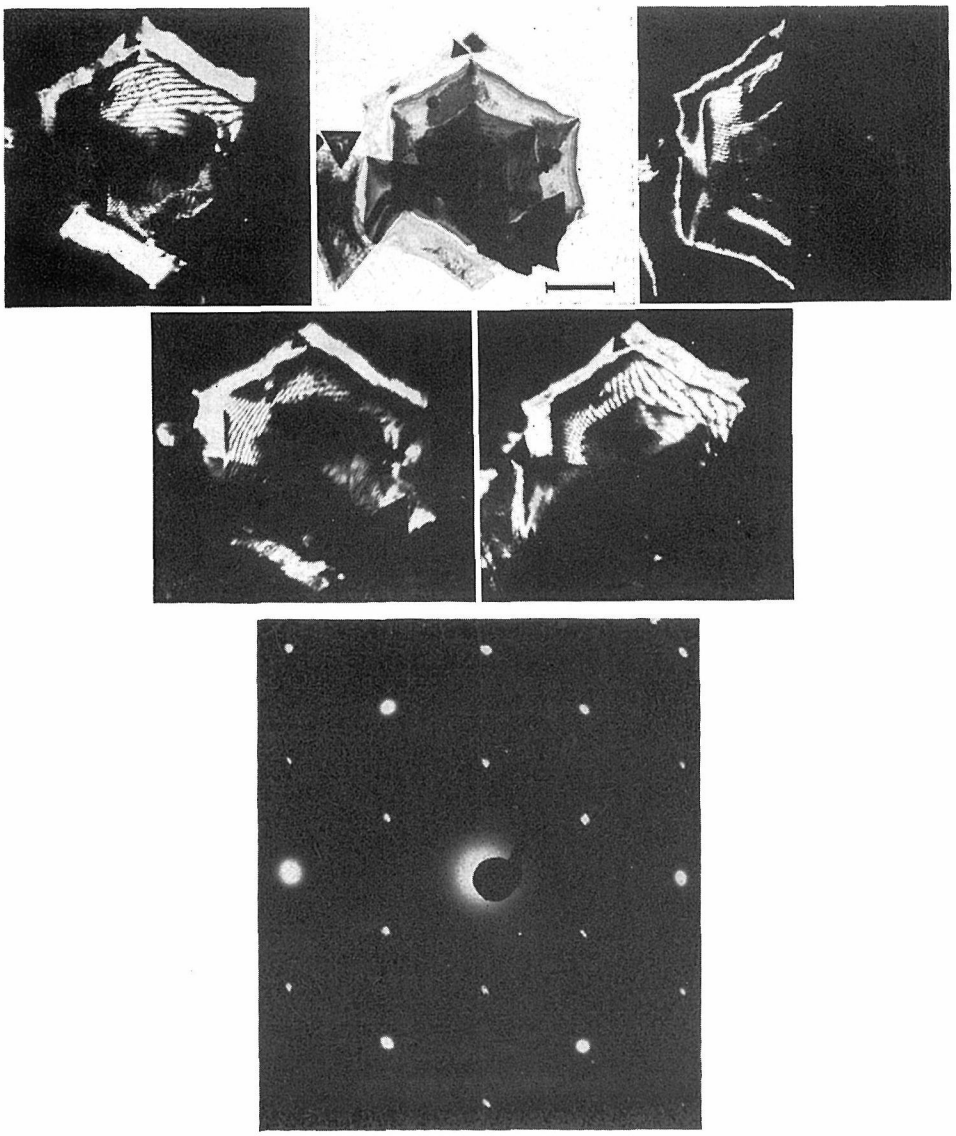

Fig. 19. The analysis of dark field images of moiré patterns for the determination of the rotational misorientations.

these holes are also observed in the carbon replicas, they are not due to the damage caused by heavy electron bombardment.

Frank[33] has derived an equation which relates the diameter (D_0) of the hole and the strength of the Burgers vector (b) at the core of the dislocation, taking it into account that, for a material having isotropic elastic constant, the free energy would be the minimum when the core is not filled up with heavily strained material but it would become an empty hole in the equilibrium state in respect to the surface energy. The equation is given as follows, though slightly modified here:

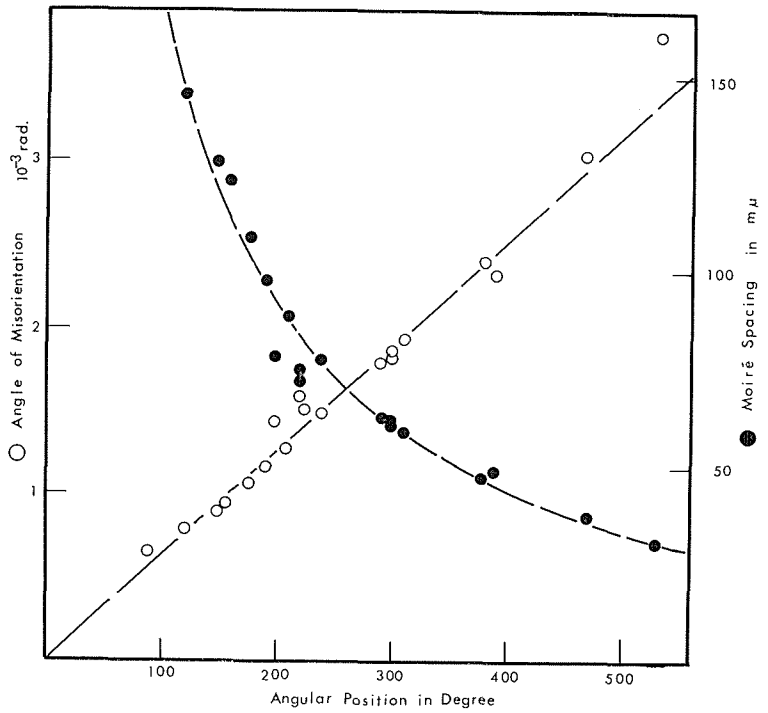

Fig. 20. Local variation of moiré fringes and rotational misorientation between steps.

$$D_0 = \frac{G}{S} \cdot \frac{b^2}{4\pi^2} \tag{4}$$

where S and G are respectively the surface free energy and the modulus of rigidity of the material. For pure gold, G and the experimental value of S are given to be 2.76×10^{11} dyne/cm^2 and 600-1000 erg/cm^2 respectively. The above relationship has been examined in the present case. The step height was measured by the shadow casting method. In the present case, comparatively complete spheres of polystyrene latex[24] prepared by Dow Chemical Corporation was used for the calibration of the magnification as well as the glancing angle of the metallic shadow.

The results are shown in Table 3. These three kinds of strengths of Burgers vectors were obtained corresponding to the three kinds of S values, that is, the upper and lower limits and the average of the two experimental values respectively. The hole diameter (D_0), the step height (h) and the shape of the spiral loop are also collected in the table.

The results show that the strength of the Burgers vector estimated by the above is in the same order as the height of the growth steps and if the latter is expected to be the actual strength of the Burgers vector or probably the bunch of Burgers vectors which make the core of screw dislocations, the equation given by Frank is also well satisfied in

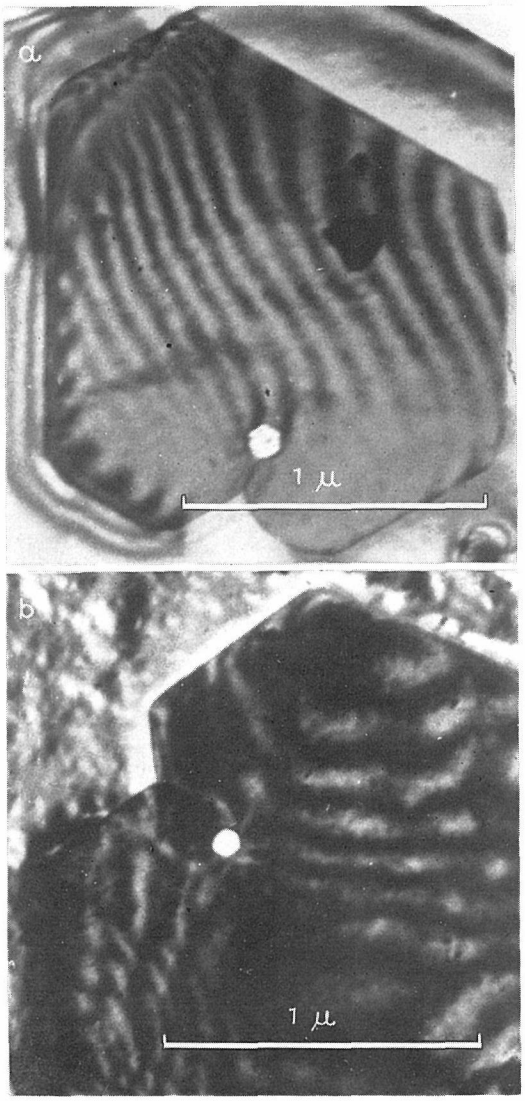

Fig. 21. The small holes at the center of the spiral loop.

Table 3.

D_0 (Å)	b_1 (Å)	b_m (Å)	b_2 (Å)	h (Å)	Shape
478	65	72	87	91	Hexagon
582	72	81	97	81	"
685	78	87	105	101	"
755	81	90	109	87	"
770	82	92	112	82	"
780	83	93	113	115	"
910	89	99	120	87	"
1045	96	107	129	103	"
3690	182	202	242	139	"
655	76	84	102	126	Trigon
664	77	85	103	123	"
844	86	96	115	120	"

the present case.

Fig. 22 is the histogram of the hole diameter, which shows that the most probable value is about 1000 Å and the mean value is about 1020 Å. The similar observation

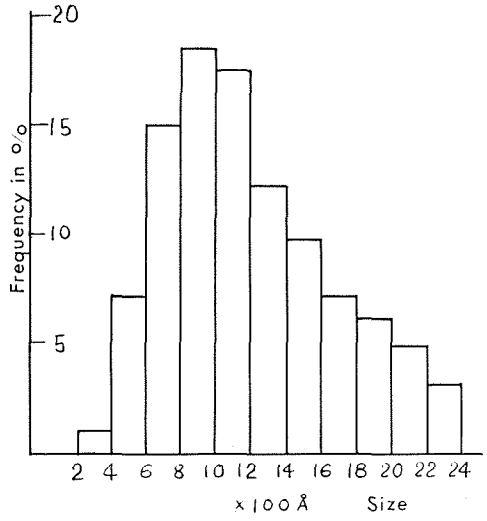

Fig. 22. The distribution histogram of the size of small holes.

was recently made by Chiang and Turkevich[8] and the results were in good agreement. The mean value of the step height turned out to be 100 Å which is in the same order as the thickness of ordinary crystals that was calculated from the subsidiary maxima of the diffraction spots. With these two values the S was calculated with the same equation as above under an assumption that the step height is equal to the strength of the Burgers vector. The result became 815 erg/cm^2 for the surface free energy, which is in turn a reasonable value for the experimentally given surface free energy of gold as reported so far[25].

The Indented Growth Front

The growth mechanism of such laminar crystals of gold in the suspension is of great interest and the intermediate stage of the growth was stepwise examined at very 24 hours by electron microscopy. The results of the observation are represented in the photographs of Figs. 23 to 25., which explicitly show the characteristic features of the growing crystals. Fig. 23 is to show the time dependence of the variation in the morphological aspect of the crystal lamella during the growth. In an earlier stage of the growth, the crystal takes an irregular form with so much crooked perimeter as is shown in Fig. 23(a) which is an example of those found in the solution during the first 24 hours. The extinction contors are rather diffuse and twisted, suggesting that the crystal itself contains heavy distortions in it. Furthermore, at several places on the crystal, these contor lines abruptly become discrete showing the existence of some dislocation at

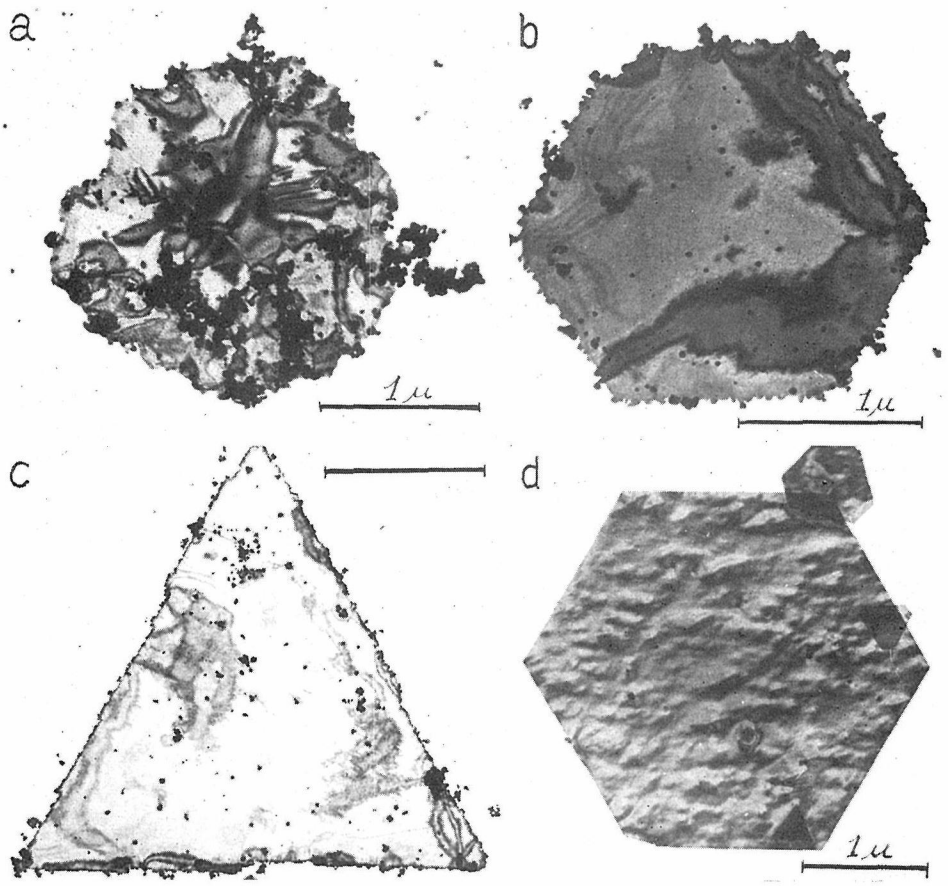

Fig. 23. Indented perimeters of growing laminar gold crystals.

these points. All these effects show that the crystals at this stage are far from being perfect not only in the outlook but also in the inner crystal structure. Small particles of about 30 mμ in diameter are sticking to the surface as well as to the indented perimeter of the crystal.

Fig. 23 (b), is the other crystal after two days elapsed in the suspension. This crystal already took a explicit form of a hexagon but the perimeter is still heavily indented as that in the above stage.

After three days, the crystals in the suspension took much more regular form as shown in Fig. 23 (c), as an example. The perimeter is still indented though less remarkable than ever.

One of the completely grown up crystals is shown in Fig. 23 (d), which takes regular shape with sharp straight edge lines on the contrary to those mentioned above. The series of these photographs suggest that the single laminar crystals of colloidal gold start with very irregular forms at the earlier stages, gradually taking regular polygonal form with indented growth front which is finally smoothened to the straight lines at the final stage of the total growth. It is not yet revealed at present stage when and how the crystals start to assume the straight perimeter. However, this phenomenon seems to

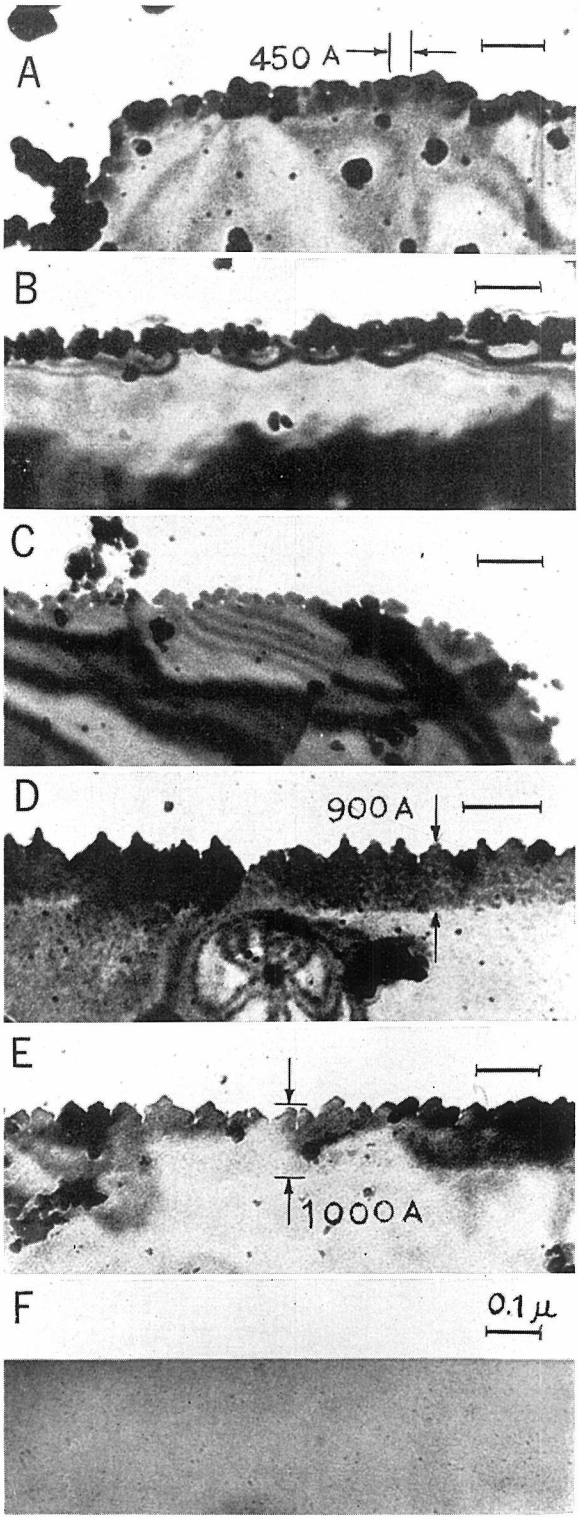

Fig. 24. Various kinds of indented perimeters.

suggest one of the most important part of the growth mechanism still left for the further investigation. During this growth, the crystal does not seem to change the thickness which has incidentally been given at the beginning of the growth. The crystal also seems to become rigid during the growth to be free from heavy distortion. A similar phenomenon was also reported recently by Chiang and Tukevich[8]. As to the indentation itself, it takes various kinds of aspects, which can be classified as shown in Fig. 24. Fig. 24 (A), shows rather round indentation, the contrast of which is the highest at the periphery of the crystal. The indentation seems due to the clinging of small colloidal particles at the periphery of the crystal. The rearrangement of the atomic row may take place through the contacting plane at the edge so as to fit itself to the lattice of the mother crystal. Fig. 24 (B) is the one densely fringed and the thickened with small particles of high contrast, the size of which is about 500 Å on an average.

Fig. 24 (C), is another type of round indentation, the thickness of which seems to be uniform everywhere. The striking feature in this case is the small holes of about 60 Å that appear very close to the perimeter. However, these holes may be completely filled out later since their appearance is restricted only to the neighborhood of the indentation and no more observed in inner part or completely grown up crystals. Fig. 24 (D) is a type where the indentation consists of many peninsulae like shark-tooth. The highly contrasted band of about 900 Å wide is left behind the perimeter toward the interior, which may be caused by the strain in the crystal lattice which is still far from the perfectness just after the new formation of the crystal. Fig. 24 (E), is similar indentations to the previous one with peninsulae of a uniform thickness and high contrast band close to the perimeter. However, the slight difference is to have more regular shape of individual peninsulae which are formed with apparent hexagonal edge lines. The direction these of edge lines are parallel to one of the $[1\bar{1}0]$, $[10\bar{1}]$ and $[01\bar{1}]$ directions, and hence per pendicular or crossing at an angle of 30° to some of the main perimeter or the whole crystal. It seems reasonable to assign the set of $(1\bar{1}0)$, $(10\bar{1})$ and $(01\bar{1})$ planes respectively to those small facets which enclose the side surface of each peninsula as shown in Fig. 25.

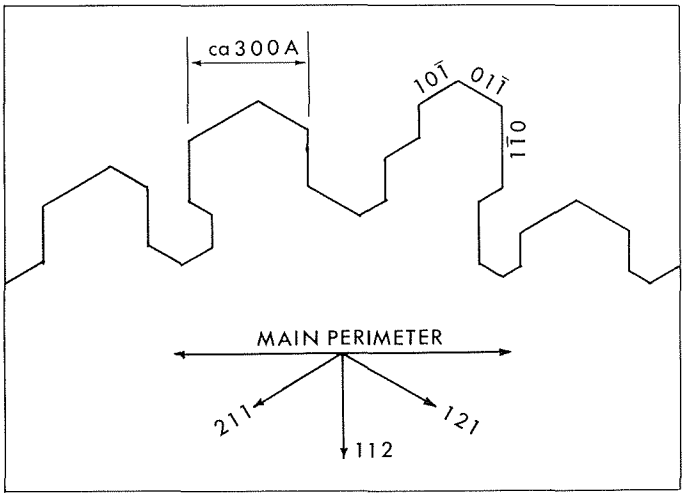

Fig. 25. Schematic diagram of a special indentation with regular hexagonal peninsulae.

The indented perimeter completely disappears at the end of crystal growth. Fig. 24 F shows an example of such a perfect straight line in order to emphasize this fact.

The indented perimeter is not an exception in the case of spiral growth. The photographs in Fig. 26 (a), shows an example of the uncompleted gold crystal with spiral

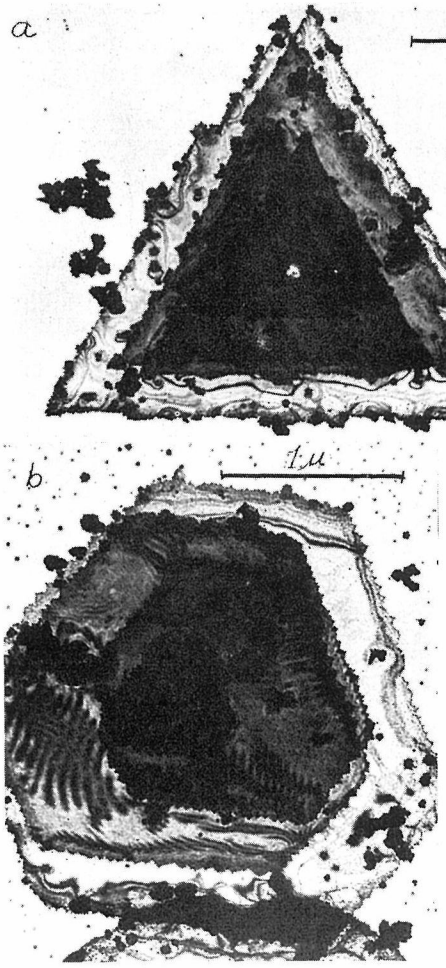

Fig. 26. Indented perimeters that appeared on growing piral steps.

steps in it. It seems apparent that the spiral growth takes place by the deposition of the mosaic unit of the crystal on every edge of the terrace of the spiral steps at the same speed. The similar mechanism was discussed by Rae and Robinson[28] in the case of the spiral growth of lithium sulfate crystal from supersaturated solution. The moiré fringes also appear on the superimposed steps but they are very diffuse and rather irregular as mentioned in the previous section.

From these results the mechanism of mosaic growth is suggested where the unit of deposition varies in size from ordinary atomic order to a usual colloidal particle of a few ten's Å. The secondary rearrangement of the lattice should take place for the deposi-

tion of the particles of larger unit.

CONCLUSION

In acidic gold sol, laminar single micro-crystal of gold grows to form a platelet with the triangular symmetry. By selected area electron diffraction, the large habit face is assigned as (111) face of f.c.c. lattice of gold, which is known to be the most closely packed plane. The thickness was calculated from the subsidiary maxima of electron diffraction spots to be 80 to 100 Å in an average. The most striking feature, however, seems to be the mechanism of the growth in the solution. The influence of the pH of the solution is very important factor. Morris and Milligan[29] also emphasized the significance of the behavior of hydrogen ions in their investigation.

As a matter of fact, the growing crystals are always accompanied by indented perimeters which finally disappear as the crystal growth comes to an end. Small particles with a similar size to the ordinary colloidal gold are also observed simultaneously in the solution, which very often stick to the perimeter of the platelet of growing gold crystal forming very thick indentations.

It has been well known that the particles of the ordinary colloidal gold sol are deposited by coagulation when strong acid is added to the stable sol such as Zsigmondy sol, Weimarn sol and Faraday sol. The condition under which these laminar crystals are formed is so much acidic that fine gold particles of ordinary size would not be stable but stick to one another to form agglomerates in the solution. Thus, it is very much comprehensive that these small particles are easy to stick to the perimeters which are the effective growth front freshly formed in the solution. Many electron micrographs suggest the possibility that the particles adsorbed on the perimeter are consumed and digested to form the new part of the mother crystal through the atomic rearrangement of the crystal lattice. More plausible assumption will be that the sticking particle is the same gold as the mother crystal and even when a considrable misfit between the both lattices takes place, this will make new screw dislocations at the contact, which in turn will be effective as the growth source for the atomic order. However, the direct proof to verify the actual mechanism is still uncovered.

The existnce of a band with higher contrast as the perimeter area is obvious from the electron microscopy, which is considered to be due to the strain in the crystal lattice, although the total configuration is the same as the inner part of the crystal since the extinction contor lines are uniform in both areas. Insomuch as this band completely disappears as time elapses, a kind of aging process accompanied by the rearrangement of crystal lattice has to be taken into consideration. The spiral growth steps that are very often observed on the crystal face is also very important factor to clarify the mechanism of the growth. When and how the indentation of the perimeters disappears at the fianl stage of the growth is also an intersting subject to be solved. These factors are still under investigation in our laboratory and the results will be reported in the near future.

REFERENCES

(1) B. von Borries and G. A. Kausche, *Koll.-Z.*, **90,** 132 (1940).
(2) E. Suito and M. Arakawa, *Report Comm. E.M.*, 56-C-17 (1951).
(3) J. Turkevich, P. Stevenson and J. Hillier, *Disc. Farad. Soc.*, **11,** 35 (1951).
(4) E. Suito and N. Uyeda, *Report Comm. E. M.*, 57-C-1 (1951).
(5) K. Miura and B. Tamamushi, *J. Electronmicros.*, **1,** 36 (1953).
(6) R. Hocart and A. Oberlin, *Mem. Sci. chim. l'Etat*, **39**, 120 (1954).
(7) B. Brüche, *Kulloid-Z.*, **170,** 97 (1960).
(8) Y. Chiang and J. Turkevich, *J. Colloid Sci.*, **18,** 772 (1962).
(9) E. Suito and N. Uyeda, *J. Electromicros.*, **1,** 33 (1953).
(10) R. P. Heidenreich, *J. Appl. Phys.*, **20,** 993 (1949).
(11) E. Suito and N. Uyeda, *Proc. Japan Acad.*, **29,** 324 (1953).
(12) E. Suito and N. Uyeda, "Proc. Intern'l Conf. E. M. London," p. 223 (1954).
(13) K. Ito and T. Ito, *J. Electronmicros.*, **1,** 18 (1953).
(14) E. Suito and N. Uyeda, *Proc. Japan Acad.*, **29,** 331 (1953).
(15) H. Hashimoto, *J. Phys. Soc. Japan*, **9,** 150 (1954).
(16) H. A. Behte, *Ann. Phys., Lpz.*, **87,** 55 (1928).
(17) F. C. Frank, *Disc. Farad. Soc.*, **5,** 48 (1949).
(18) S. Amelinkx, *Phil. Mag.*, **43,** 5 2 (1952).
(19) E. Suito and N. Uyeda: *Nature*, **185,** 453 (1960); "Forth Intern'l Conf. on E. M., Berlin", **1,** 355 (1958).
(20) E. Suito and N. Uyeda, *J. Electronmicros.*, **8,** 25 (1960).
(21) H. Poppa and O. Rang, *Z. Phys.*, **153,** 643 (1959).
(22) S. Amelinckx and E. Votova, *Nature*, 172, 538 (1953).
(23) F. C. Frank, *Acta Cryst.*, **4,** 497 (1951).
(24) E. B. Bradford and J. W. Vanderhoff, *J. Appl. Phys.*, **26,** 864 (1955).
(25) W.E, Garner, "Chemistry of the Solid State", p. 116 (1955).
(26) E. Suito and N. Uyeda, *Proc. Japan Acad.*, **37,** 388 (1961).
(27) H. Uyeea, *J. Electronmicros.*, **10,** 170 (1961).
(28) H. Rae and A. E. Robinson, *Proc. Roc. Soc.*, **A222,** 558 (1954).
(29) R. H. Morris and W. O. Milligan, *J. Electronmicros.*, **8,** 17 (1960).